Materials Science & Engineering B 248 (2019) 114408

Contents lists available at ScienceDirect

Materials Science & Engineering B

journal homepage: www.elsevier.com/locate/mseb

Ferroelectric polarization and fatigue characterization in bismuth-based Aurivillius thin films at lower voltage

J. Yang[a], D.P. Song[b,*], Y. Yin[c], L.Z. Chen[a], L.-Y. Chen[b], Y. Wang[b], J.Y. Wang[a,*]

[a] School of Materials Science and Engineering, Jiangsu University of Science and Technology, Zhenjiang 212003, PR China
[b] Department of Physics, Jiangsu University of Science and Technology, Zhenjiang 212003, PR China
[c] Division of Electronics and Informatics, Gunma University, Kiryu, Gunma 376-8515, Japan

ARTICLE INFO

Keywords:
Pb-free
Aurivillius phase
Fatigue
Thin film

ABSTRACT

One of significant issue in ferroelectrics is so called "size effect", that is ferroelectric properties may disappearance at a finite critical thickness, especially those films prepared by solution process. Here, the reliable polarization fatigue resistance and retention performance of chemical solution deposited Aurivillius family thin films $Bi_6Fe_2Ti_3O_{18}$ with thickness down to 90 nm and at low driving voltage are reported. Intrinsic ferroelectricity is insight and verified by PUND measurement, and further research demonstrate that it can compared with other thicker films. In addition, the voltage-dependence fatigues feature in $Bi_6Fe_2Ti_3O_{18}$ films have been demonstrated. Considerable remanent polarization 18.9 $\mu C/cm^2$ and lower operating voltage 6 V make it not only as a promising ferroelectric material in memory application; it also endows non-vacuum solution process as a good alternative for ultrathin ferroelectric films.

1. Introduction

Most common feature of ferroelectric materials is that their spontaneous polarization can be switched by applied electric field excessed the coercive field [1]. The scaling of such polarization reversing with size is considered to be one of the fundamental issues in ferroelectrics research, which has been received extensive and intense concern. The focus of attention is at a critical dimension that the ferroelectric performance will disappear, or not [2]. Essentially, ferroelectric polarization loop is a collected electrical signal during the reversal of ferroelectric domain, which originated from the spontaneous breaking of the pristine symmetry [3]. The domain structure can be "seeing" by force microscopy, while the hysteresis loops may "reading" by electrical measurement. On one hand, based on the perspective of basic research and benefit from the fast developments of film deposition technology, some research group can be growth unit cell-level thickness ferroelectric films [4,5]. Usually, piezoelectric microscopy or electric force microscopy are used to determination their ferroelectricity, i. e. "seeing" the domain structure [6]. On the other hand, from the perspective of device application and driven by the trend of device miniaturization, ferroelectric ultrathin films (typical thickness below 100 nm) have been attracted of great interests [7]. Generally, the polarization loop can be obtained, i. e. "reading" the domain reversed by collected electrical signal. Almost all of them are based on vacuum process, such as PLD (pulsed laser deposition), MBE (molecular beam epitaxy), MOCVD (metal organic chemical vapor deposition), ALD (atomic layer deposition) and magnetron sputtering et al. CSD (chemical solution deposition) as a widely used method in ferroelectric thin films preparation are also gained extensive attention, but the thickness of the derived films are rarely less than 100 nm [8,9]. The cause of this phenomenon is not only from the intrinsic lack of thickness control of CSD, but also from the difficulties of performance characterization, i. e. lose of hysteresis loops result from "reading" process failure.

When lead's toxicity became more and more pressing, the true trouble with lead is that it is so useful [10]. Regardless of the piezoelectric properties, however, ferroelectric materials that can contend against PZT have been developed in bismuth layered Aurivillius oxides [1]. Bismuth layered Aurivillius oxides of generic formula $Bi_2A_{n-1}B_nO_{3n+3}$ is made of several (n) perovskite-like $A_{n-1}B_nO_{3n+1}$ blocks alternating with fluorite-like Bi_2O_2 layers along the c-axis [11,12]. Typically, the A-site (12-coordinated) and the B-site (6-coordinated) is occupied by mono-, di- or trivalent cations and by d-orbital tetra-, penta- or hexavalent cations, respectively, such as K^+, Sr^{2+}, $Bi^{3+}Ln^{3+}$, and Ti^{4+}, $Nb^{5+}W^{6+}$. The Aurivillius families include a larger number of ferroelectrics based on the above components; some of them have been extensively studied as fatigue-free ferroelectrics for their potential used in nonvolatile memories. The case of non-d-orbital cations like Fe^{3+}, Co^{3+}, Ni^{3+}, Cr^{3+}, Ru^{4+}, Ir^{4+} or Mn^{4+} at the B site has also been

* Corresponding authors at: Department of Physics, Jiangsu University of Science and Technology, Zhenjiang 212003, PR China.
E-mail addresses: dpsong@just.edu.cn (D.P. Song), jywang@just.edu.cn (J.Y. Wang).

https://doi.org/10.1016/j.mseb.2019.114408
Received 9 October 2018; Received in revised form 21 June 2019; Accepted 13 August 2019
Available online 21 August 2019
0921-5107/

considered in the search for magnetic and multiferroic Aurivillius phases [13–16]. $Bi_6Fe_2Ti_3O_{18}$ as one of such Aurivillius compounds are expected coexisting of ferroelectric and magnetic ordering that show spontaneous magnetization and polarization simultaneously at ambient conditions. The magnetic ground state has been demonstrated belongs to paramagnetic with the presence of a short-range antiferromagnetic ordering, but fortunately well-defined ferroelectric was achieved by process optimization CSD recently [17,18]. This paves the way to investigate the thickness dependence of the ferroelectric properties as mentioned above. It was surprising that the well-defined ferroelectric–hysteresis loops can remained after the thickness less than 100 nm. The sub-100 nm ferroelectric loop was very scarce in the previous literature in CSD films. It is not only important in fundamental physics research thickness dependence ferroelectric properties, but also interesting in ferroelectric-based device application compatible with existing standard silicon integration circuit technology.

To clarify the ferroelectric properties of the $Bi_6Fe_2Ti_3O_{18}$ thin films with thickness reducing, in this work, we investigated the ferroelectric behavior of $Bi_6Fe_2Ti_3O_{18}$ thin film with thickness below 100 nm and prepared by the chemical solution deposition method [19]. The thickness dependence of the ferroelectric properties, such as remanent polarization P_r, is presented. Moreover, fatigue and retention properties are indeed inspect as a crucial factors in determining the performance and longevity of ferroelectric based devices. The external electric field amplitude dependence fatigue and retention properties of the BFTO thin films were also investigated.

2. Experimental details

Thin films of $Bi_6Fe_2Ti_3O_{18}$ (BFTO) were fabricated on polycrystalline Pt/Ti/SiO_2/Si substrate by chemical solution deposition route in ambient atmosphere with rapid annealing process. The required stoichiometric high-purity bismuth acetate, iron acetate and tetrabutyl titanate was dissolving in propanoic acid under vigorously stirring. Besides, a 5 mol% excess amount of bismuth acetate was used to compensate the volatilization of bismuth in the thermal processing. The resulting precursor solution was spin-coated 20 s at 6000 rpm and then baked 10 min in a 400 °C preheated tube furnace. Process of spin-coating and pyrolysis was repeated several times in order to get a desired thickness. The dried film was amorphous and subsequently crystallized in tube furnace for 30 min at 700 °C. The sheeny and crack-free films were adhered well on the substrate.

The room-temperature crystal structure of derived films was determination by use a Philips XPert PRO X-ray diffractometer (XRD, Philips, Holland) equipment Cu-Kα radiation. The microstructure, surface morphology and thickness of the films were checked by a high resolution transmission electron microscopy (HR-TEM, JEM-2010, JEOL Ltd, Japan) and a field emission scanning electron microscopy (FE-SEM, Sirion 200, FEI Company, USA). The measurements of X-ray photoelectron spectroscopy (XPS, VG Scientific, ESCALAB250, USA) were done by using Al K_α to obtain the valence state information of the ions in BFTO thin films. The dielectric properties were measured in the frequency range of 20 Hz–1 MHz using a driving voltage of 1 V by a precision LCR meter (TH2828/A/S model, China). Ferroelectric properties were measured using a computer-controlled standardized ferroelectric test system (Precision Premier II, Radiant Technology, USA). Top Au electrodes were sputtered by a shadow mask for electrical properties measurement.

3. Results and discussion

3.1. Phase and microstructure analysis

Fig. 1 shows the XRD patterns of BFTO with various film thicknesses and the inset Fig. 1(a) shows the magnified results of low angle 2θ from 10 to 35° for clarity. The results indicate that the samples are of pure

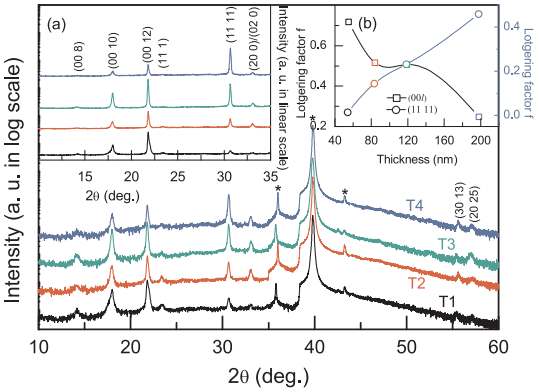

Fig. 1. Crystalline structure characteristics of the investigative Aurivillius films with different thickness: T1 55 nm, T2 90 nm, T3 120 nm and T4 200 nm. (a) The enlargement of low angle XRD patterns. (b) The variations in the Lotgering factor (f) of (00l) and (1111) peak with the thickness. The asterisk represents the diffraction peak of the substrate.

Aurivillius layered structures without detectable impurity phases, and the pattern of the samples can be indexed with an orthorhombic lattice with the space group *B2cb*, which is in agreement with the previous results [20]. Indeed, the (020) diffraction peak cannot be distinguished from the (200) peak for all samples suggest that reliable orthorhombic rather tetragonal phase is fabricated. Additionally, the relative diffraction intensity of (1111) peak located at θ ~30° of all derived BFTO films exhibit a persistent increasing with thickness increased, while the relative diffraction intensity of (0012) peak located at θ ~22° show inverse tendency in the Fig. 1(a). It is indicting that the growth rate of (00l)-oriented grains lower than the (1111)-oriented grains. The thickness dependence orientations have been observed in Aurivillius Phase, which evident anisotropy ferroelectric in such compounds [21]. To make it clearly, the Lotgering factor (f) was calculated to estimate the degree of (1111) and c-orientation using the following formula: $f = (P - P_0)/(1 - P_0)$, where $P_0 = \sum I(00l)/I(hkl)$ indicates the proportion of (00l) intensities to the total (hkl) intensities for a randomly oriented films and P indicates the intensity proportion for a specified sample. $f = 0$ and $f = 1$ indicate random and full texture, respectively. The corresponding results are show in the inset (b) of Fig. 1, they gave obvious inverse tendency.

Usually, layer structure materials are preferred to c-axis orientation growth, such as high temperature superconductor$YBa_2Cu_3O_7$, thermoelectric material $Bi_2Sr_2Co_2O_y$ and $Ca_3Co_4O_9$, due to lower out-plane surface energy [22]. This growth model is also agreeing to lower n Aurivillius phase $Bi_4Ti_3O_{12}$, it can easily be grown with the c-axis result in the so-called c-axis orientation films. Unfortunately, a negligible polarization component along the film normal in such c axis–oriented films, because the major spontaneous polarization vector of these lower n Aurivillius phase materials is along the a axis [23]. Another aspect is that the electrical conductivity along the a-axis is lower several orders of magnitude than that along the c-axis samples. Taking into account the effects of polarization and leakage current together, to some degree (11 11) or c-axis preferred BFTO ultrathin films in this study may favorable to “reading” hysteresis loop in detail below.

Further insights to the layer structures of derived films are implementation by use the HR-TEM, due to the close XRD peak position for Aurivillius structures with adjacent $(A_{n-1}B_nO_{3n+1})^{2-}$ layers. Take T4 as an example, a long-term periodic layered structure can be visualized in HR-TEM image, as shown in Fig. 2(a). The Fig. 2(b) given the further clearer HR-TEM in order to distinguish the layered structure and compared with the schematic diagram of their crystallographic structure. Homogeneous four perovskite layers sandwiched by two $(Bi_2O_2)^{2+}$ layers crystal structure are directly confirmed, which is consistent to the observation in other Aurivillius compounds reported before [24]. It is

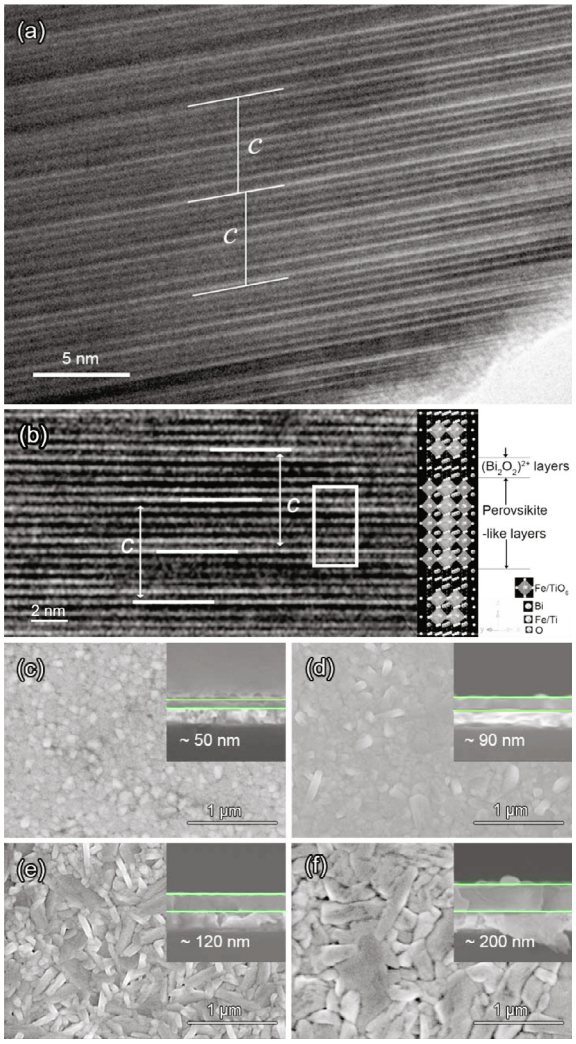

Fig. 2. (a) and (b) The representative HR-TEM image of layer structure and corresponding schematic diagram of unit cell structure. The lines as a visual guide of periodicity. Perovskite ferroelectric layers are intergrowth with rock dielectric layers are clearly. Surface and cross-section of FE-SEM results for the BFTO thin films: (b) T1 55 nm, (c) T2 90 nm, (d) T3 120 nm, (e) T4 200 nm.

well establishing that the perovskite ferroelectric layers are intergrowth with rock dielectric layers. The lattice constant *c* of the T4 thin film is to be 4.973(2) nm and 4.962(3) nm obtained from the HR-TEM and XRD results, respectively, which shown close to earth other. Note that the TiO_6 and FeO_6 octahedron are indistinguishable under used measuring environment, e. g. Ti and Fe element are random occupied in B-site of Aurivillius perovskite-like layers.

Surface and cross-section of FE-SEM results for all BFTO thin films are given in the lower part of Fig. 2. Both the grain (particle) size and film thickness are increased clearly. The growth of grain (particle) is quite obviously with thickness increase, and all films seems possess different surface morphology. The annealing treatment of thin films is a process of nucleation and growth. Under rapid annealing conditions, the films first nucleate rapidly and then grow. The process of grain growth is the result of continuous phagocytosis and consumption. For the thinner films, there are large number of nucleation sites in the plane. Once the adjacent grains swallow each other and growth, they will form a particle-like morphology as T1. For the thicker films, the more nucleation sites in the vertical direction lead to the larger the grain size during the growth process. In the growth process, on the one hand, the grain size increases, on the other hand, there will be some voids. These two points are exhibit in the SEM pictures. Aurivillius ceramics with plate-like grains are usually observed because of the larger anisotropic nature of the crystallographic structure [13]. Meanwhile, the grain-like morphological appear in the present thin films can be attributed to that the low processing temperature of films compared to their ceramics counterpart. The increased crystallite/grain size will play a role in determination of thin film properties as discussed below. The increased thickness is the result of deliberately design, which is approximately 55, 90, 120, 200 nm and all profile-section of films looks similar.

3.2. Dielectric and leakage properties

The frequency dependence of dielectric and voltage dependence of leakage current performances for BFTO thin films are shown in Fig. 3(a) and (b), respectively. In the Fig. 3(a), with the increase of frequency, the relative dielectric constant ε_r and dielectric loss tanδ exhibit an overall decreasing trend except the tanδ of T2 film. At a constant frequency, the ε_r increases and the tanδ decreases with increasing the thickness. For instance, the value of ε_r increases from 112 to 154 and tanδ decreases from 0.2 to 0.04 at 1 MHz when the films thickness increases from 90 to 200 nm. The room temperature leakage current in a semi-log scale on the electric voltage (I-V) curves for BFTO thin films shown monotonically decreases with increasing the film thickness and the current decreases several orders of magnitude from 3.29×10^{-3} (T1 films, 55 nm) to 9.41 9 3.16×10^{-7} A (T4 films, 198 nm). Such thickness dependence dielectric and leakage properties have been observed in the much ferroelectric and can accepted from films orientation, domain structure and grain size et al [25–27]. Different orientations of films and grain size may take mainly responsible to dielectric variation as exhibit in Fig. 3(a). However, film thickness is dominated as display in Fig. 3(b) even c-orientation films have lower electrical conductivity, thus the film of T1 reveal considerable leakage current.

3.3. Ferroelectric polarization properties

Fig. 4 shows the polarization-voltage (P-V) and remnant polarization-voltage (R-V) hysteresis curves of various thicknesses BFTO films under electric field of about 700 kV/cm (T2, T3) and 500 kV/cm (T4), simultaneously the corresponding displacement current- voltage (I-V) curves were also recorded. The thicker thin films display a rectangular hysteresis loop with a considerable remnant polarization compared with T1 thin film. The values of P_r in T2, T3, T4 samples are 18.9 μC/cm^2, 16.9 μC/cm^2 and 18.8 μC/cm^2, respectively. These values are compared to lanthanide doped $Bi_4Ti_3O_{12}$ and larger than that in $SrBi_2Sr_2O_9$ thin film, which are mostly evaluated as a lead-free ferroelectrics used in nonvolatile FeRAM [27,28]. Those values are also comparable

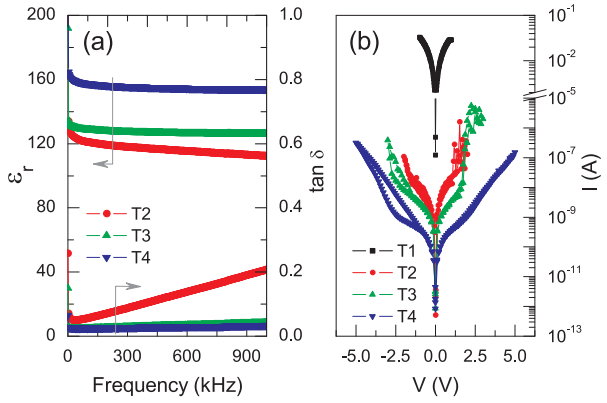

Fig. 3. Room temperature dielectric and leakage results: (a) frequency dependence of dielectric constant (ε_r) and dielectric loss (tanδ) of thin films, and (b) leakage current I-V curves in semi-log scales for all films.

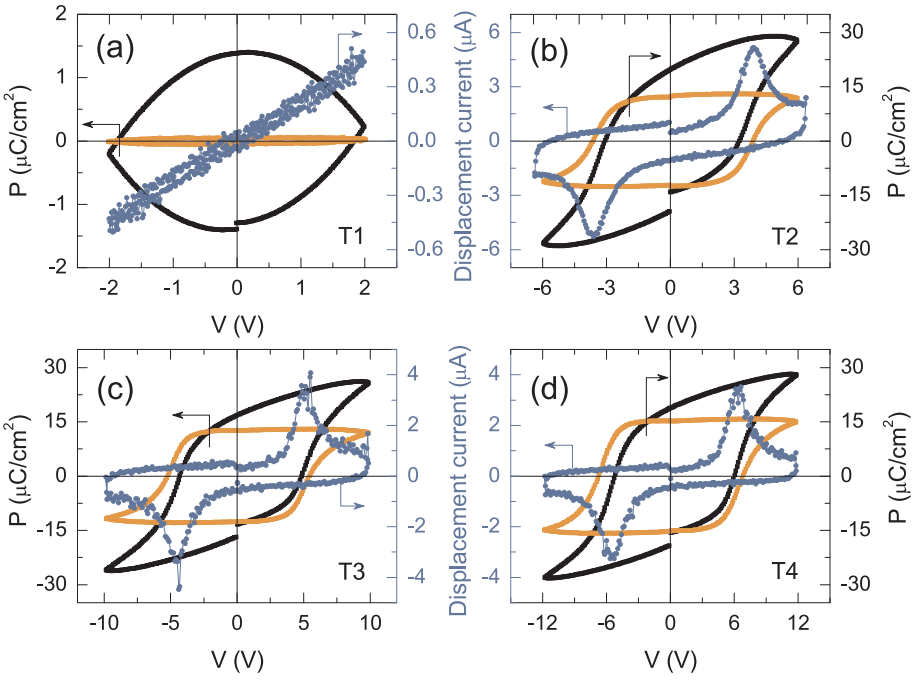

Fig. 4. Room temperature ferroelectric hysteresis loops based on the normal bipolar measurement (black line) and the PUND method (yellow line) for thin films of (a) T1, (b) T2, (c) T3, and (d) T4. Displacement current-voltage (blue line) curve recorded during the bipolar measurement. For linear resistor (or suffer leakage ferroelectrics), a linear relationship clearly between the current and voltage. In contrast, there are obvious current peaks with increasing the applied voltage amplitude in the case for a real ferroelectric sample.

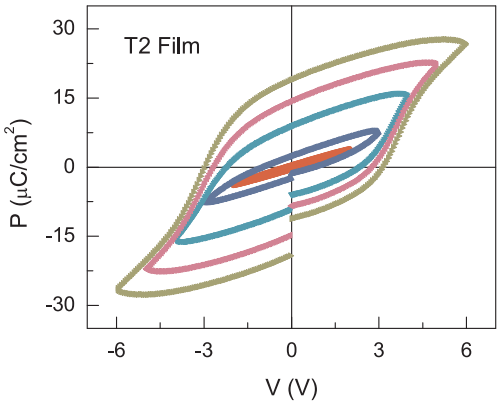

Fig. 5. P-V hysteresis loops of the T2 sample measured under different applied electric fields.

to P_r of Co-doped $Bi_6Fe_{1.4}Co_{0.6}Ti_3O_{18}$ thin films (~17.6 μC/cm^2) and V-doped $Bi_{5.97}Fe_2Ti_{2.91}V_{0.09}O_{18}$ thin film (~16.4 μC/cm^2) reported before [29,30]. Note that the saturation polarization P_s of all thicker films present an approximate value of 30 μC/cm^2, indict that P_s independent of film thickness. The P-V loop of sample T1 given a typical curve of linear resistor that displacement current keeps the same phase with voltage, representing a linear relationship between them as show in the corresponding Fig. 4(a) [3]. That means the T1 sample has not ferroelectricity or seriously the ferroelectricity can not "reading" by such testing approach which main caused from larger leakage in such thickness. Piezoresponse force microscopy, one of the most effective approaches to evaluate the nanoscale ferroelectric domains, can introduced to characterized the ferroelectric properties of such film, but it is not the context of this writing. Beside of this, to eliminate non–-hysteresis components contributed to P-V loop in ferroelectric thin films, the Positive-Up Negative-Down (PUND) measurement, which extract only the hysteresis component automatically without any assumptions, are performed [31]. By PUND method, the remanent polarization–electrical voltage (R-V) hysteresis loops of all derived thin films are also shown in Fig. 4. R-E loops received by PUND are rather squareness and no obvious polarization gap exists between the starting and ending electric field besides T1 film. Also, there is no measurable remanent polarization in the film of T1, which evident by horizontal straight line in Fig. 4(a).

For T2, T3 and T4 films in Fig. 4(b), (c) and (d), the squareness and symmetrical R-E hysteresis loops with remanent polarization P_R of 12.2 μC/cm^2, 12.6 μC/cm^2 and 15.3 μC/cm^2 are identified. Combination the Fig. 2(c) and Fig. 4(b), it is remarkable that well-defined ferroelectric loop and intrinsic hysteresis contribution can obtained when thickness of film down to 100 nm. Furthermore, displacement current-voltage curves displayed in Fig. 4(b) confirm the ferroelectric response, because the current maxima do not occur at the maxima of electric voltage. In fact, relating to the maximum current is identical to the V_c determined by the P-V loop, related to the domain reversal. Only the maximum current generated by the domain reversal or switching is the sign of ferroelectric [3]. The displacement current–voltage curves of T3 and T4 films are demonstrate in the Fig. 4(c) and (d), further confirmed the intrinsic ferroelectricity.

In order to give a clear relation between polarization and electric fields amplitude, various fields amplitude hysteresis loop tests were carried out. The P-V hysteresis loops of T2 thin film with applied electric fields is shown in the Fig. 5. Other thin films have analogous polarization characteristics namely polarization is positively related to electric field. The robust ferroelectric properties present in the ultrathin film accompanied by lower operate voltage (around 5 V) show some application prospect. The external electric field E = V/d, where V and d are external voltage and film thickness, can be easy realized to exceed coercive field by reduce the thickness of sample below to 100 nm. For example, 5 V voltage go to electric field of 600 kV/cm in T2 film, which is almost twice the coercive field of such ferroelectric. Due to the thickness of the bulk ferroelectric, the operate voltage of several kilovolts is required to switch the capacitors that impede application in microelectronic device in a long period of time [32]. It should be note that, a monotonically rising trend of P_Rs is different to non-monotonic transition of P_rs as the thickness increases. The ratio of non–hysteresis components (calculate by $\Delta P = (P_r - P_R)/P_r \times 100\%$) is 35.4%, 25.4%, and 18.6% for T2, T3, and T4, respectively. It can derivate that hysteresis components are increased with thickness increasing. Effect of thickness on remanent polarization is various in perovskite ferroelectric and bismuth layered ferroelectric. There are results include decrease [25], independent [26] and increase [27] with thickness increasing. As derived films, the thickness dependence remanent polarization main

attribute to different leakage contribution and the effective electric field to the films. For thinner film T2, larger P_r and non–hysteresis ratio can be explained by larger leakage current compared to thicker counterpart. Note that, hysteresis circuits do not measure polarization directly in practical measurement. Actually, they measure switched charge Q. The switched charge for an ideal ferroelectric insulator is following as: $Q = 2P_rA$, where A is the electrode area of a film capacitor configuration. While for a slightly conductive sample: $Q = 2P_rA + \sigma E_a t$, whereσ, E_a and t is the electrical conductivity, applied field and measuring time, respectively [33].

It is obvious that conductivity will make the value of P_r lager. After deduct the non-hysteresis components by PUND test, it share the similar value of P_R with T3 film. While for the T4 sample, the effective electric field applied to the films could be larger than those thinner films due to smaller leakage current, which result in larger P_r and P_R. On the other hand, in addition to access to large electric field, film texture is easier to control make it possess striking differences properties compare to the bulk counterpart. Ferroelectric film with the vector of the spontaneous polarization perpendicular to substrate is desired, which will produce better polarization effect. As a results from XRD in Fig. 1, (00l) orientation is decrease gradually while (1 1 11) orientation show gradually increasing trend. Consideration the direction of spontaneous polarization in Aurivillius ferroelectric is along a-axis, film of T4 will obtained preferable polarization due to the relative intensity of strongest peak transform from (0 0 12) to (1 1 11). It is also accepted that the properties of ferroelectric thin film are deeply affects by grain size and grain boundary. Film of T4 has significant grain size compared to other two films, which make the ferroelectric properties of T4 capacitor more advanced and stable than the other two capacitors.

3.4. Ferroelectric fatigue and retention properties

Besides the intrinsic and robust ferroelectric polarizations are demonstrated, ferroelectric reliability issues, such as polarization fatigue (a decrease in polarization with repeated switching) and retention (stability of the remnant polarization with time) properties are also concerned when it faces to any practical application [1]. Below, derived film's reliability issues are examined. The sample of T1 is not considered in this section as a result of the ferroelectric polarization hysteresis loop become invalid for the capacitor.

Fig. 6(a) given the polarization fatigue-endurance performances of derived films except T1. In order to comparison of clear, normalized polarization is used. Bipolar pulses switching voltage of 4, 5, 6 V at 10 kHz and a test voltage of 6, 8, 10 V at 5 kHz were carry out to fatigue testing of T2, T3 and T4 film, respectively. The polarization loss is approximately 23% for T3 and T4, however, no obvious polarization loss appears in T2 film capacitor up to 10^7 switching cycles. The P-V and R-V curves of Fig. 6(b), (c) and (d)) were obtained at a certain applied voltage before and after the electrical fatigue test. Polarization degeneration are clearly in last two samples, whatever by conventional or PUND method. The R-V results suggest that i) the polarization loss is intrinsic because reduced P_R, ii) non-hysteresis components is insensitive to fatigue due to similar decline amplitude. Besides, the V_c of three films becomes small after fatigue test, which have been reported before in other ferroelectrics [34].

There is a view that fatigue is a competing between the pinning and de-pinning of domain walls, rather than any fundamental reduction of the polarization [33]. Certainly, based on locate phase decompose has also been propose to explain fatigue phenomenon in perovskite ferroelectrics [35]. In addition, electrode damage and microscopic or macroscopic crack form as a result in fatigue has also been observed in films and bulk ferroelectrics. After fatigue testing, we found that the electrode has not been damaged in film capacitors configuration, and no crack form under SEM. Under the locate phase decompose model, the degenerated polarization should be irreversible unless re-annealing in a previous crystallization temperature to regrowth of initial phase. While based on domain wall pinning model, the virgin remanent polarization of the fatigued film can be restored under larger field after fatigue, because de-pining occurs in this condition and fundamental polarization unaltered [36]. Following this principle, two kinds of test have been performed on T4 film i) fatigue test in different switching voltage with 10 kHz and ii) larger applied voltage is used to P-V loop measured after fatigue. The results are present in Fig. 6(e) and (d). As see in Fig. 6(e), the degrees of fatigue increased with voltage increasing to 6 V, but alleviate to further increase the voltage. In the low voltage regimes (V = 2, 4 V less than V_c = 5.6 V), exhibits a little polarization fatigue. In the medium voltage regimes (V = 5, 6 V nearby V_c), serious fatigue phenomenon appeared. In the high voltage regimes (V = 8 V), the speed of fatigue decreased and show revert in some degree. This voltage-dependence fatigue feature has been research in lower n Aurivillius phase, such as SBT and BiT [37,38]. The domain boundaries can constitute strong electrostatic potential wells suggest by Dimos et al. [39]. After trap charges at such a domain boundary, the domain is pinned result in reducing the switchable polarization.

On the other hand, pinned domains could be released by switching cycles has also been discussed in detail by Zhong et al., which cause an increase of P_r[38]. The fatigue behavior of ferroelectrics based on such pining and de-pining model has been explained by space charge such as oxygen vacancy ($V_o^{\cdot\cdot}$) $V_o^{\cdot\cdot}$ in previous research reports. It is agree that $V_o^{\cdot\cdot}$ is one of the major defects in perovskite-related ferroelectrics. Usually, the $V_o^{\cdot\cdot}$ may formed at the annealing process because the evaporation of volatile element, such as bismuth in Aurivillius compounds. It can be express as the below equation: $2Bi_{Bi} + 3O_o \rightarrow 2V_{Bi}^{'''} + 3V_o^{\cdot\cdot} + Bi_2O_3$. The present high temperature and ambient annealing process imply that the generation of $V_o^{\cdot\cdot}$ is inevitable.

Beside of this, the XPS measurement is also demonstrated the coexistence of Fe^{2+} and Fe^{3+} in the present film. The XPS spectra of thin films show in the Fig. 7, the Fe $2p_{3/2}$ can be split into two peaks by the Gaussian-Lorentzian curve fitting, which shows the existence of Fe^{2+} and Fe^{3+} ions based on the peak location of 710.04 eV and 711.28 eV [40]. In this case, in order maintain the charge neutrality origin from the frustration of Fe^{2+} and Fe^{3+} ions oxygen vacancies induced through the Kröger–Vink relation: $2Fe^{3+} + 1/2\ O_o \Leftrightarrow 2Fe^{2+} + V_o^{\cdot\cdot}$ Where O_o is the null oxygen, $V_o^{\cdot\cdot}$ is the oxygen vacancy with two positive charges. The $V_o^{\cdot\cdot}$ related domain pining and de-pining model could explain fatigue behavior of the present film. Rejuvenation of polarization as demonstrate in the Fig. 6(f) after apply a high applied voltage further exclude locate phase decompose model. There are three P-V loops in the Fig. 6(f), which are fresh, fatigued and rejuvenated. The first two loops represent the results before and after fatigue. The last one is the result both after the fatigue test is completed and then under the excitation of large electric field. Actually, large electric field used here is more than 600 kV/cm (about 12 V) and it should be repeated several times for stability. Finally, the little polarization degeneration of T2 film as shows in the Fig. 6(a) can be ready clarify. The better fatigue resistance observed can attribute to the higher probability of oxygen vacancy de-pining under higher voltage amplitudes (4 V approach to 500 kV/cm for T2 sample), which makes it more difficult to pining the domain walls. On the other hand, Table 1 was the summary of the P_r, P_R, ratio of non–hysteresis components and fatigue decreasing in the below table for clearly comparison. The main reason of the P_r obtained in T2 larger than T3 is that T2 thin film has larger non–hysteretic contribution due to its high leakage current as shown in the Fig. 3(b). It can be seeing that the non-hysteresis components ratio decreases monotonously from T2 to T4, lead to monotonic increases of P_R. All those values suggest that T4 thin film have more intrinsic contributions of polarization domains reverse and show more obvious fatigue phenomenon of after cyclic switching test. As there are more non–hysteretic parts (35.4% mentioned above), T2 films show smaller polarization loss after fatigue testing because such non–hysteretic parts do not change during test.

Fig. 8 shows the polarization-retention characteristic and related polarization hysteresis loops of derived films except T1. Polarization-

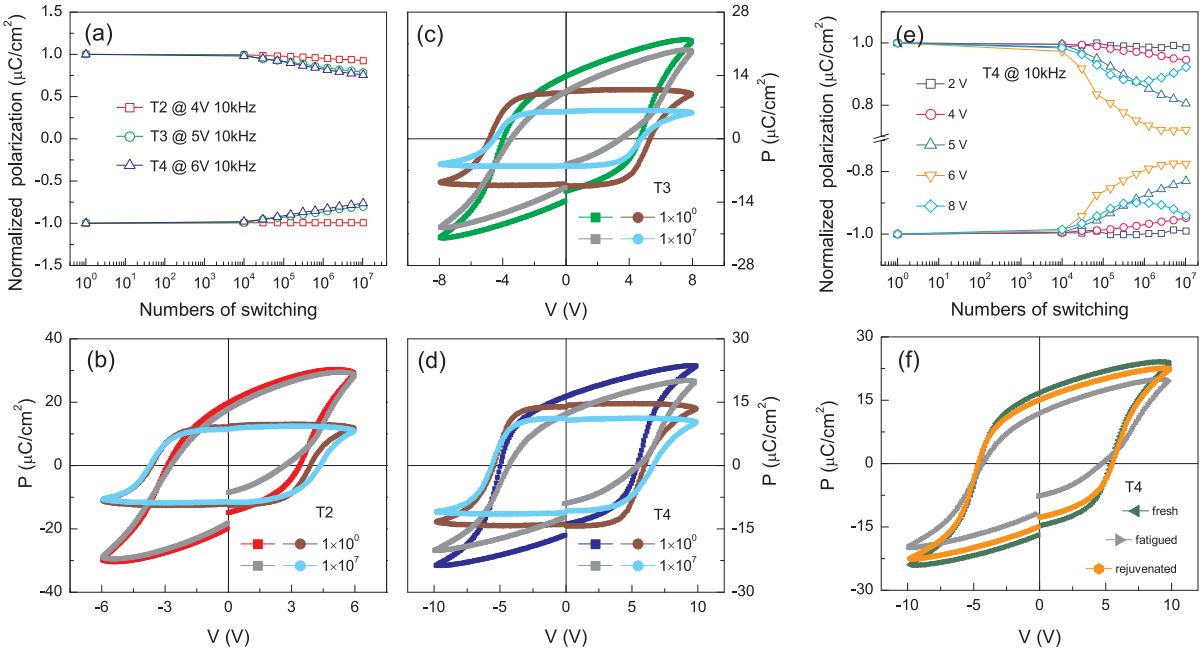

Fig. 6. Electrical fatigue characteristics of the BFTO capacitors before and after being subjected to 1×10^7 read/write cycles at a frequency of 10 kHz. (a) The normalized fatigue test results of T2, T3 and T4 by a selected fatigue and measuring voltage. (b) P-V and R-V hysteresis loops measured before and after the switching cycle for T2. Similarly, results of T3 and T4 are given in (c) and (d). (e) The normalized fatigue test results of T4 under different applied voltage and (f) polarization rejuvenation after high applied voltage stimulation.

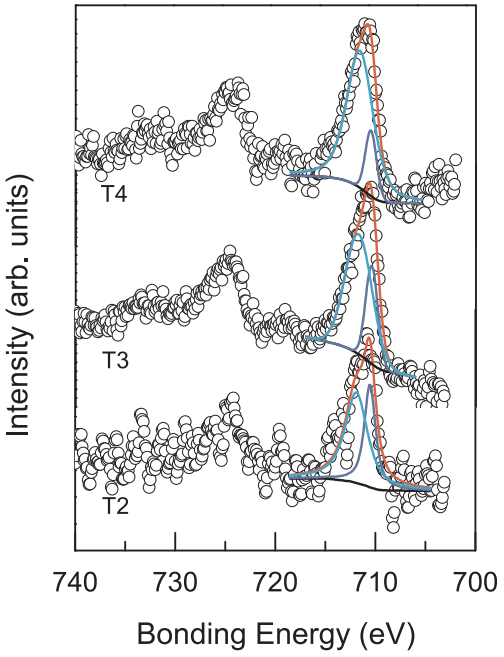

Fig. 7. The XPS spectra of thin films result indicate that the coexistence of Fe^{2+} and Fe^{3+}.

Table 1
The summary of the P_r, P_R, ratio of non-hysteresis components and P_r decreasing after fatigue.

0.9	P_r μC/cm²	P_R μC/cm²	Ratio (%)	Fatigue (%)
T2	18.9	12.2	35.4	8
T3	16.9	12.6	25.4	23
T4	18.8	15.3	18.6	25

retention test pulse sequence is illustration inset of Fig. 8(e). An increase in non-switching polarization ($P^\wedge$ and $P_r^\wedge$) or decrease in switching polarization (P^* and P_r^*), or they occurs simultaneously will caused a reduce of remanent polarization (expressed as $\Delta P = P^* - P^\wedge$ or $P_r^* - P_r^\wedge$). Both switching and non-switching polarization values show a slight upward trend in T2 film (see Fig. 8(a)), it is suppressed in thicker films T3 and T4 (see Fig. 8(c) and (e)). However, the retained switchable polarization (namely ΔP) of all samples are rather stable during a retention time of 2×10^4 s. The appearance of upward may cause from the conductivity of thinner film compared to others and high pulse voltage used (5 V standard Si integrated circuit operating voltage, which is approach to 600 kV/cm for T2 sample). After a retention time of 2×10^4 s, the polarization loss was ignorable compared with the value measured at t = 1 s at a certain amplitude of applied electric field. The P-V and R-V ferroelectric loops are record before and after the retention test. The corresponding hysteresis loops was almost identical as shown in the Fig. 8(b), (d) and (f) for three films, further evident that no loss of the switchable polarization. It is also implied that the structures have little or no tendency to imprint after retention test, which is in accordance with the results of fatigue test. Formation of charged domain walls and nonswitchable domains has been proposed as an origin of retention loss in PZT ferroelectric thin films [41]. However, Both P-V and R-V hysteresis loops record after fatigue and retention test indicate that such nonswitchable domain is insignificant in films. Depolarization fields, usually generated by defects and dipole charges or the redistribution of space charge, and is considered as the mechanisms for the polarization decay after writing. In perovskite-related ferroelectric materials, long-term retention losses is occurs usually due to the existing of charged defects V_o, which cause depolarization fields result in polarization weakening. However, this effect leads to a small decrease in the polarization by compensating the polarization charges when the redistribution of defect charges is driven by polarization [42]. In present film, larger switched charge could compensate the charged defects effect on the polarization loss during the retention times.

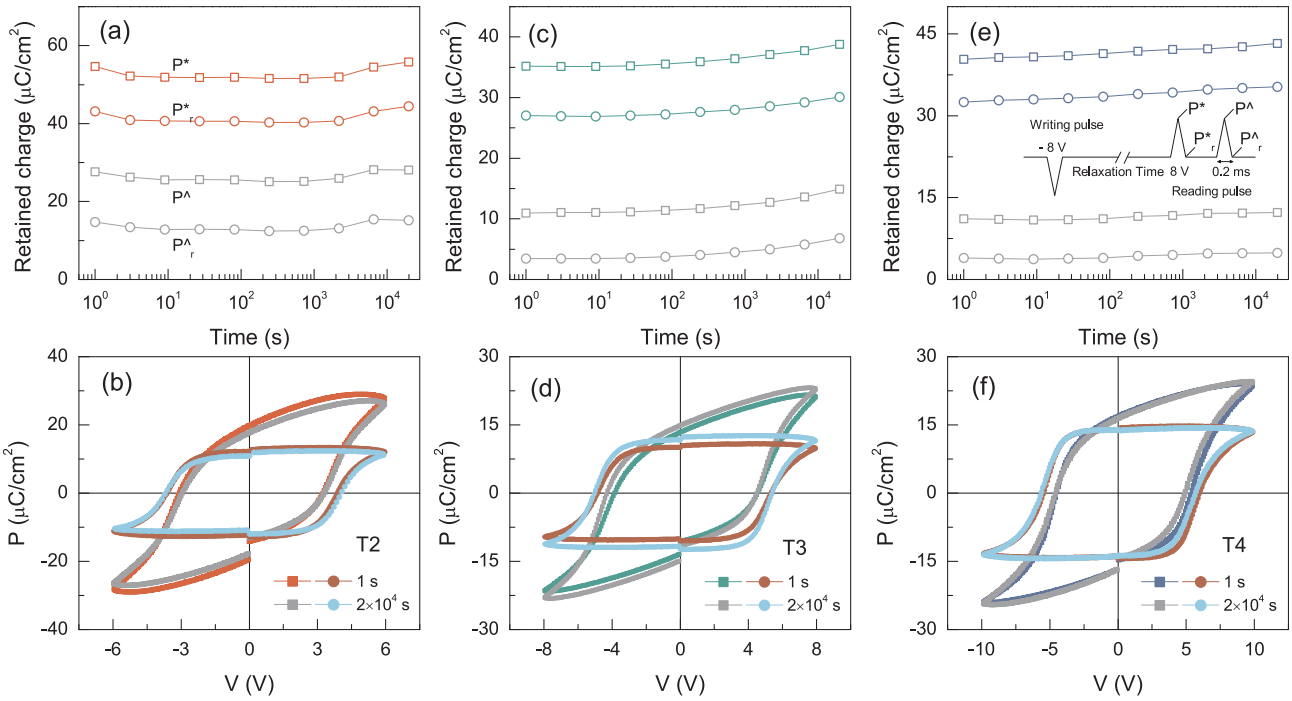

Fig. 8. Charge-retention characteristics of the BFTO capacitors plotted as a function of time after the application of a writing pulse: (a) T2, (c) T3 and (e) T4. Polarization-retention test pulse sequence is illustration inset (e), note that the writing and reading voltage is just used in T4 film. Corresponding P-V and R-V hysteresis loops measured before and after the 1×10^4 s waiting time show below of them: (b) T2, (d) T3 and (f) T4. The symbol of P^*, $P^\wedge$, P_r^*) and $P_r^\wedge$) are explained in main text detail.

4. Conclusions

In summary, ferroelectric $Bi_6Fe_2Ti_3O_{18}$ ultrathin films were prepared by chemical solution deposition. The detailed investigation of the ferroelectric polarization properties and fatigue characterization were carrying out. Significantly, ferroelectric polarization loops with reliable polarization fatigue resistance and retention performance are demonstrated in film with thickness down to 100 nm. Intrinsic ferroelectricity is insight and verified by PUND measurement, and it can have compared with other thicker films. The sub-100 nm film has commensurable ferroelectric parameters to their thicker counterparts, but a lower operating voltage (can work under 5 volts). The voltage-dependence fatigue feature has been demonstrated, and the mechanism of fatigue is proposed as the oxygen vacancy relevant domain wall pinning model. The availability of these new ferroelectric features is important for basic physics research and for future device development. The results provide a candidate to search lead-free ferroelectric thin film and room temperature multiferroic in Aurivillius phase with good ferroelectric properties.

Declaration of Competing Interest

The authors declare that they have no known competing financial interests or personal relationships that could have appeared to influence the work reported in this paper.

Acknowledgements

This work was supported by the National Natural Science Foundation of China (Grants No. 51801077, 11847093) Jiangsu Education Committee (No. 17KJB140006) and the Scientific Research Foundation of JUST (Nos. 1052931611, 1052921801).

References

[1] J.F. Scott, Applications of modern ferroelectrics, Science 315 (2007) 954–959.
[2] J. Junquera, P. Ghosez, Critical thickness for ferroelectricity in perovskite ultrathin films, Nature 422 (2003) 506–509.
[3] L. Jin, F. Li, S. Zhang, D.J. Green, Decoding the fingerprint of ferroelectric loops: Comprehension of the material properties and structures, J. Am. Ceram. Soc. 97 (2014) 1–27.
[4] D. Lee, H. Lu, Y. Gu, S.Y. Choi, S.D. Li, S. Ryu, T.R. Paudel, K. Song, E. Mikheev, S. Lee, S. Stemmer, D.A. Tenne, S.H. Oh, E.Y. Tsymbal, X. Wu, L.Q. Chen, A. Gruverman, C.B. Eom, Emergence of room-temperature ferroelectricity at reduced dimensions, Science 349 (2015) 1314–1317.
[5] J.A. Mundy, C.M. Brooks, M.E. Holtz, J.A. Moyer, H. Das, A.F. Röbola, J.T. Heron, J.D. Clarkson, S.M. Disseler, Z. Liu, A. Farhan, R. Held, R. Hovden, E. Padgett, Q. Mao, H. Paik, R. Misra, L.F. Kourkoutis, E. Arenholz, A. Scholl, J.A. Borchers, W.D. Ratcliff, R. Ramesh, C.J. Fennie, P. Schiffer, D.A. Muller, D.G. Schlom, Atomically engineered ferroic layers yield a room-temperature magnetoelectric multiferroic, Nature 537 (2016) 523–527.
[6] L.J. McGilly, P. Yudin, L. Feigl, A.K. Tagantsev, N. Setter, Controlling domain wall motion in ferroelectric thin films, Nat. Nanotechnol. 10 (2015) 145–150.
[7] D. Meng, S. Tao, H. Huang, J. Wang, Y. Yun, R. Peng, Z. Fu, L. Zheng, S. Chu, W. Chu, X. Zhai, G. Brown, R. Knize, Y. Lu, Discerning lattice and electronic structures in under- and over-doped multiferroic Aurivillius films, J. Appl. Phys. 121 (2017) 114107.
[8] X. Obradors, T. Puig, M. Gibert, A. Queralto, J. Zabaleta, N. Mestres, Chemical solution route to self-assembled epitaxial oxide nanostructures, Chem. Soc. Rev. 43 (2014) 2200–2225.
[9] Y. Bastani, T. Schmitz-Kempen, A. Roelofs, N. Bassiri-Gharb, Critical thickness for extrinsic contributions to the dielectric and piezoelectric response in lead zirconate titanate ultrathin films, J. Appl. Phys. 109 (2011).
[10] P. Ball, Stealing a lead on lead, Nat. Mater. 9 (2010) 98.
[11] N.A. Benedek, J.M. Rondinelli, H. Djani, P. Ghosez, P. Lightfoot, Understanding ferroelectricity in layered perovskites: new ideas and insights from theory and experiments, Dalton Trans. 44 (2015) 10543–10558.
[12] P. Fang, C. Zhi, Z. Xi, W. Long, X. Li, Giant dielectric response at low frequency of B-site modified Aurivillius oxide potassium bismuth titanate, Mater. Res. Bull. 108 (2018) 214–218.
[13] W. Gu, X.N. Li, S.J. Sun, L.Y. Zhu, Z.P. Fu, Y.L. Lu, Magnetocrystalline anisotropy in the Co/Fe codoped Aurivillius oxide with different perovskite layer number, J. Am. Ceram. Soc. 101 (2018) 2417–2427.
[14] C.H. Wang, Z.F. Liu, L. Yu, Z.M. Tian, S.L. Yuan, Structural magnetic and dielectric properties of $Bi_{5-x}La_xTi_3Co_{0.5}Fe_{0.5}O_{15}$ ceramics, Mater. Sci. Eng., B 176 (2011) 1243–1246.
[15] D.P. Song, J. Yang, Y.X. Wang, J. Yang, X.B. Zhu, Magnetic and ferroelectric properties of Aurivillius phase $Bi_7Fe3Ti3O_{21}$ and their doped films, Ceram. Int. 43 (2017) 17148–17152.

[16] N.A. Lomanova, I.V. Pleshakov, M.P. Volkov, V.V. Gusarov, Magnetic properties of Aurivillius phases $Bi_{m+1}Fe_mTi_3O_{3m+3}$ with m = 5.5, 7, 8, Mater. Sci. Eng., B 214 (2016) 51–56.
[17] J. Yang, W. Tong, Z. Liu, X.B. Zhu, J.M. Dai, W.H. Song, Z.R. Yang, Y.P. Sun, Structural, magnetic, and EPR studies of the Aurivillius phase $Bi_6Fe_2Ti3O_{18}$ and $Bi_6FeCrTi3O_{18}$, Phys. Rev. B 86 (2012) 104410.
[18] D. Song, J. Yang, B. Yang, L. Chen, F. Wang, X. Zhu, Evolution of structure and ferroelectricity in Aurivillius $B_4Bi_{n-3}Fe_{n-3}Ti_3O_{3n+3}$ thin films, J. Mater. Chem. C 6 (2018) 8618–8627.
[19] N. Bassiri-Gharb, Y. Bastani, A. Bernal, Chemical solution growth of ferroelectric oxide thin films and nanostructures, Chem. Soc. Rev. 43 (2014) 2125–2140.
[20] T. Jia, H. Kimura, Z. Cheng, H. Zhao, Effects of substrate temperature on the microstructure and ferroelectric properties of Aurivillius $Bi_6Fe_2Ti3O_{18}$ thin films, J. Alloys Compd. 632 (2015) 473–477.
[21] G.D. Hu, S.H. Fan, X. Cheng, Anisotropy of ferroelectric and piezoelectric properties of $Bi_{3.15}Pr_{0.85}Ti3O_{12}$ thin films on Pt(100)/Ti/SiO_2/Si substrates, J. Appl. Phys. 101 (2007) 054111.
[22] X.B. Zhu, D.Q. Shi, S.X. Dou, Y.P. Sun, Q. Li, L. Wang, W.X. Li, W.K. Yeoh, R.K. Zheng, Z.X. Chen, C.X. Kong, (001)-oriented $Bi_2Sr_2Co_2O_y$ and $Ca3Co_4O_9$ films: self-assembly orientation and growth mechanism by chemical solution deposition, Acta Mater. 58 (2010) 4281–4291.
[23] H.N. Lee, D. Hesse, N. Zakharov, U. Gosele, Ferroelectric $Bi_{3.25}La_{0.75}Ti3O_{12}$ films of uniform a-axis orientation on silicon substrates, Science 296 (2002) 2006–2009.
[24] H. Zhao, K. Cai, Z. Cheng, T. Jia, H. Kimura, Z. Ma, Q. Fu, Z. Huang, T. Matsumoto, T. Tohei, N. Shibata, Y. Ikuhara, A novel class of multiferroic material, Bi_4Ti3O_{12}-nBiFeO3 with localized magnetic ordering evaluated from their single crystals, Adv. Electron. Mater. 3 (2017) 1600254.
[25] D. Song, X. Tang, B. Yuan, X. Zuo, J. Yang, L. Chen, W. Song, X. Zhu, Y. Sun, Thickness dependence of dielectric, leakage, and ferroelectric properties of $Bi_6Fe_2Ti3O_{18}$ thin films derived by chemical solution deposition, J. Am. Ceram. Soc. 97 (2014) 3857–3863.
[26] J.P. de la Cruz, E. Joanni, P.M. Vilarinho, A.L. Kholkin, Thickness effect on the dielectric, ferroelectric, and piezoelectric properties of ferroelectric lead zirconate titanate thin films, J. Appl. Phys. 108 (2010).
[27] F. Yang, F. Zhang, G. Hu, Z. Zong, M. Tang, Thickness-dependent ferroelectric behavior of predominantly (117)-oriented $Bi_{3.15}Nd_{0.85}Ti3O_{12}$ thin-film capacitors, Appl. Phys. Lett. 106 (2015) 172903.
[28] C.-P. De Araujo, J. Cuchiaro, L. McMillan, M. Scott, J. Scott, Fatigue-free ferroelectric capacitors with platinum electrodes, Nature 374 (1995) 627–629.
[29] Z. Liu, J. Yang, X.W. Tang, L.H. Yin, X.B. Zhu, J.M. Dai, Y.P. Sun, Multiferroic properties of Aurivillius phase $Bi_6Fe_{2-x}Co_xTi_3O_{18}$ thin films prepared by a chemical solution deposition route, Appl. Phys. Lett. 101 (2012) 122402.
[30] D.P. Song, J. Yang, B. Yuan, X.Z. Zuo, X.W. Tang, L. Chen, W.H. Song, X.B. Zhu, Y.P. Sun, Improved ferroelectric polarization of V-doped $Bi_6Fe_2Ti3O_{18}$ thin films prepared by a chemical solution deposition, J. Appl. Phys. 117 (2015) 244105.
[31] Y.S. Chai, Y.S. Oh, L.J. Wang, N. Manivannan, S.M. Feng, Y.S. Yang, L.Q. Yan, C.Q. Jin, K.H. Kim, Intrinsic ferroelectric polarization of orthorhombic manganites with E-type spin order, Phys. Rev. B 85 (2012) 184406.
[32] O. Auciello, J.F. Scott, R. Ramesh, The physics of ferroelectric memories, Phys. Today 51 (1998) 22–27.
[33] M. Dawber, K.M. Rabe, J.F. Scott, Physics of thin-film ferroelectric oxides, Rev. Mod. Phys. 77 (2005) 1083–1130.
[34] X.J. Lou, H.J. Zhang, Z.D. Luo, F.P. Zhang, Y. Liu, Q.D. Liu, A.P. Fang, B. Dkhil, M. Zhang, X.B. Ren, H.L. He, Effect of polarization fatigue on the Rayleigh coefficients of ferroelectric lead zirconate titanate thin films: experimental evidence and implications, Appl. Phys. Lett. 105 (2014) 102907.
[35] X.J. Lou, M. Zhang, S.A.T. Redfern, J.F. Scott, Local phase decomposition as a cause of polarization fatigue in ferroelectric thin films, Phys. Rev. Lett. 97 (2006) 177601.
[36] X.J. Lou, Polarization fatigue in ferroelectric thin films and related materials, J. Appl. Phys. 105 (2009) 024101.
[37] D. Wu, A.D. Li, H.Q. Ling, T. Yu, Z.Q. Liu, N.B. Ming, Fatigue study of metalorganic-decomposition-derived $SrBi_2Ta_2O_9$ thin films: The effect of partial switching, Appl. Phys. Lett. 76 (2000) 2208–2210.
[38] N. Zhong, P.-H. Xiang, Y.-Y. Zhang, X. Wu, X.-D. Tang, P.-X. Yang, C.-G. Duan, J.-H. Chu, Polarization fluctuation behavior of lanthanum substituted Bi_4Ti3O_{12} thin films, J. Appl. Phys. 118 (2015) 104102.
[39] H.N. Al-Shareef, D. Dimos, T.J. Boyle, W.L. Warren, B.A. Tuttle, Qualitative model for the fatigue-free behavior of $SrBi_2Ta_2O_9$, Appl. Phys. Lett. 68 (1996) 690.
[40] X. Liu, L. Xu, Y. Huang, C. Qin, L. Qin, H.J. Seo, Improved photochemical properties of Aurivillius $Bi_5Ti3FeO_{15}$ with partial substitution of Ti^{4+} with Fe^{3+}, Ceram. Int. 43 (2017) 12372–12380.
[41] M.G. Han, M.S. Marshall, L. Wu, M.A. Schofield, T. Aoki, R. Twesten, J. Hoffman, F.J. Walker, C.H. Ahn, Y. Zhu, Interface-induced nonswitchable domains in ferroelectric thin films, Nat. Commun. 5 (2014) 4693.
[42] A.Z. Simoẽs, M.A. Ramirez, N.A. Perruci, C.S. Riccardi, E. Longo, J.A. Varela, Retention characteristics in $Bi_{3.25}La_{0.75}Ti3O_{12}$ thin films prepared by the polymeric precursor method, Appl. Phys. Lett. 86 (2005) 112909.